# Influence of spark plasma sintering and baghdadite powder on mechanical properties of hydroxyapatite

Khandan, A.; Karamian, E.; Mehdikhani-Nahrkhalaji, M.; Mirmohammadi, H.; Farzadi, A.; Ozada, N.; Heidarshenas, B.; Zamani, K.

**DOI**
10.1016/j.mspro.2015.11.087

**Publication date**
2015

**Document Version**
Final published version

**Published in**
Procedia Materials Science

Available online at www.sciencedirect.com

ScienceDirect

Procedia Materials Science 11 (2015) 183 – 189

Procedia Materials Science

www.elsevier.com/locate/procedia

5th International Biennial Conference on Ultrafine Grained and Nanostructured Materials, UFGNSM15

# Influence of Spark Plasma Sintering and Baghdadite Powder on Mechanical Properties of Hydroxyapatite

A. Khandan[a,*] , E. Karamian[b], M. Mehdikhani-Nahrkhalaji[c], H. Mirmohammadi[e], A. Farzadi[f], N. Ozada[a], B. Heidarshenas[a], K. Zamani[b]

[a]*Mechanical Engineering Department, Eastern Mediterranean University, Gazimağusa, TRNC, Via Mersin 10 Turkey*
[b]*Advanced Materials Research Center, Department of Materials Engineering, Najafabad Branch, Islamic Azad University, Najafabad, Isfahan, Iran*
[c]*Department of Biomedical Engineering, Faculty of Engineering, University of Isfahan, Iran*
[d]*Dental Materials Research Center, Department of Restorative Dentistry, Isfahan University of Medical Sciences, Isfahan, Iran*
[e]*Department of Cariology Endodontology Pedodontology, Academic Centre for Dentistry Amsterdam (ACTA), Universiteit van Amsterdam and Vrije Universiteit, Netherlands*
[f]*Department of Biomedical Engineering, Faculty of Engineering, University of Malaya, 50603 Kuala Lumpur, Malaysia*

**Abstract**

Since hydroxyapatite-based materials have similar composition and crystallinity as natural calcified tissues, can be used for bone/tissue engineering. In the present study a novel nanocomposite based on bioceramics such as Natural Hydroxyapatite (NHA) and Baghdadite (BAG), was sintered by spark plasma sintering (SPS) technique. The prepared composite was characterized using scanning electron microscopy (SEM), X-ray diffractometer (XRD) and Brunauer–Emmett–Teller (BET) techniques. The porosity of the samples was measured by Archimedes method. The cold crushing strength (CCS) test was applied to evaluate their mechanical properties. Our results demonstrated that NHA-30wt. %BAG nanocomposite specimens have the lower CCS in comparison with other examined composites. Consequently, NHA/BAG samples exhibited acceptable mechanical properties and could be suitable candidates for bone tissue engineering applications especially orthopaedic fields.



Peer-review under responsibility of the organizing committee of UFGNSM15

*Keywords:* Baghdadite; Natural hydroxyapatite; Nanocomposite; Spark Plasma Sintering; Tissue Engineering.

* Corresponding author. Tel.: 00905338529577 ; fax: 00905338529577.
*E-mail address:* amir_salar_khandan@yahoo.com


Peer-review under responsibility of the organizing committee of UFGNSM15
doi:10.1016/j.mspro.2015.11.087

## 1. Introduction

During the past several years there has been considerable interest in the bone grafting which is the main concern in biomaterials engineering, Burchardt et al. (1983). Considering serious health problems including bone degradation and tumor disorder, it is crucial need to obtain composite with predictable performance. Bone regeneration is an important issue, where discovering the suitable substitute/materials for bone graft, Finkemeier et al. (2002). However, the issues of allografting are complicated and leading to some drawbacks such as decreased bioactivity and increased risk in non-immunogenicity, Khandan et al. (2014). Those materials designed to induce tissue reactions for bonding or those used to deliver drugs are usually bioactive, Ramaswamy et al. (2008), Khandan et al. (2015). Sinterability, solubility rate and mechanical properties may depend on the chemical and physical nature of material including its extent of crystallinity, crystallite size, processing condition and porosity, Ramaswamy et al. (2008). The chemical composition of calcium phosphates (CaPs) controls dissolution rate of the implanted bones. According to literature, the presence and the type of ions have a vital role influencing bioactivity, osteoblast growth, materials performance, Wu and Chang (2004).The substitution of Zn, Mg, Ti and Zr into CaPs enhanced the bioactivity and mechanical performance of biomaterials, Ramaswamy et al. (2008), Lu et al. (2013). Considering the brittleness and high porosity of bioceramic materials, calcium zirconium silicate (CZS) ceramics have been developed to overcome these drawbacks by Al-Hermezi et al. (1987) to use in orthopedics, bone regenerative and dentistry application, Ramaswamy et al. (2008). Incorporation of Zr ions into CZS structure was investigated by Ramaswamy et al. (2008), and a stable Ca–Si based material was obtained. Among the calcium-based bioceramics baghdadite is a series of silicates (BAG: $Ca_3(Zr)Si_2O_9$) has an excellent *in-vitro* biological properties in terms of possessing good bioactivity, apatite-formation abilityand capable of stimulate the cell growth, Karamian et al. (2014). It is not well explored biomaterial therefore its physical, mechanical and biological properties need to be detailed investigated, Khandan et al. (2015). There are numerous studies regarding to bioactive HA which has a good osteoconductivity and used as bulk bioceramics, Farzadi (2014), coatings, and granules in surgery and clinical applications, but biodegraded in blood plasma quickly.

**Nomenclature**

| | |
|---|---|
| W | Initial Weight |
| E | Young's modulus |
| F | Force (N) |
| A | Area (m2) |

## 2. Materials and methods

### *2.1. Preparation of NHA*

An NHA is produced by hydrothermal process derived from young Calf bone. The wet bone were cleaned by acetone and heated at 110°C in the atmospheric furnace for 2 hours. Then, burned pieces were crushed into small pieces by high energy planetary ball milling (HEBM) process with 400 rpm speed and ball to powder rate (BPR) 10:1which is cleaned by acetone and dried with compressed hot air. Therefore, the homogenized NHA were purified.

### *2.2. Preparation of BAG*

The mixture of calcium carbonate ($CaCO_3$) (99%, Merck-Germany), zirconium dioxide ($ZrO_2$) (99%, Merck-Germany), and silicon dioxide ($SiO_2$) (98%, Merck-Germany) with a molar ratio of 3:1:2, which corresponds to the stoichiometric composition of pure BAG. Powders were blended and mixed by mechanical activation (MA) process. The HEBM process was chosen to avoid segregation of oxides under a BPR of 15 and a vial velocity of 400 rpm for

10 h. The mixture of raw materials was calcined at 1100, 1200 and 1350°C for 2, 3, and 4 h with a heating rate of 10°C/min. Synthesis parameters for the BAG by MA method through HEBM process are illustrated in table 1.

### *2.3. Preparation of the nanocomposite*

The NHA powders with crystal size of less than 2 µm were selected to composite with BAG. The composites with different amounts of BAG (10 wt.%, 20 wt.% and 30 wt.%), was mechanically activated through HEBM process. The product was uniaxially pressed at 90 MPa pressure in cylindrical mould with a dimension of 6×20 mm (diameter × height). The powders were weighed in amounts of 0.65 g and pressed in cylindrical shape for 4 min under 8000 N force to compress uniformly.

Table 1. Parameter used to synthesis the BAG with MA method through HEBM.

| Step | Ball milling time (h) | Ball weight (g) | Powder weight (g) | Temperature (°C) | Similar peak (%) | sintering (h) |
|---|---|---|---|---|---|---|
| 1 | 10 | 86.5 | 10 | 1100 | 35% | 2-3 |
| 2 | 10 | 80.0 | 10 | 1200 | 40% | 3-4 |
| 3 | 10 | 90.5 | 10 | 1350 | 65% | 3-4 |

### *2.4. Sintering process of the nanocomposite*

Sintering of the nanocomposite was carried out with spark plasma sintering (SPS) process by using SPS furnace (Nabertherm, Germany Co, Malekeashtar University Isfahan, Iran). The bulk ceramics were put into a die of carbon and heated to a predetermined temperature at a heating rate of 200°C/min, at the same time; a pressure of 50 MPa was applied. After dwelling for 5 min, the pressure was released and the sample was cooled to below 650°C in 4 min.

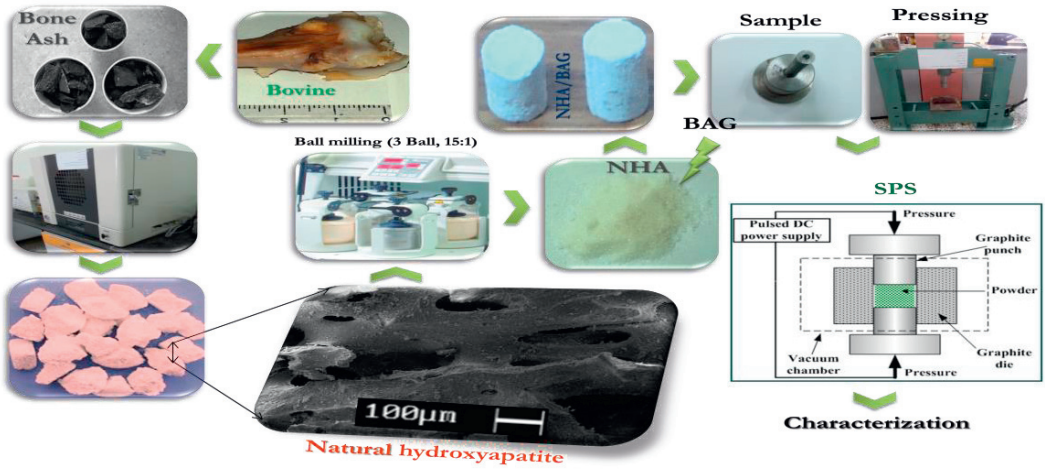


Fig. 1. Schematic of the preparation of the nanocomposite, and sample characterization.

The porosity of ceramic spheres before SPS was measured according to Archimedes' principle; 1.5 g of spheres in water was used to measure their open-pore porosity. The porosity was calculated according to the following Eq. 1

$$Porosity = \frac{(W2 - W1)}{W2 - W3)} \times 100\%, \quad (1)$$

Where $W_1$ is the weight of composite in air, $W_2$ is the weight of sample with water, and $W_3$ is the weight of samples suspended (soaked) in water. The CCS test was determined by crushing cylindrical specimens of dimensions 10×20 mm (diameter×thickness) using a computer-controlled universal testing machine (Instron 8874, UK: performed in EMU, Turkey). The Young's modulus (E) and last compressive stress (σ) data were calculated. The standard No. of CCS test in ASTM is C0020-00R05 to monitor the CCS of the fabricated samples. According to the diameter (d) of the sample, the following (Eq. 2) is used**:**

$$CCS \left(\frac{kg}{cm2}\right) = \frac{F}{A} = \frac{F}{\frac{\pi d2}{4}} \quad (2)$$

Comparison of CCS and percentages of apatite formation in all nanocomposites are summarized in Table 2.

## 3. Materials characterization

The porosity of the samples was measured by Archimedes method. Their mechanical properties were identified by CCS test. SEM analysis evaluations were performed using a Philips XL30 (Eindhoven, the Netherland) to investigate the surface morphology of sample which is sintered by SPS process. TEM analysis (Philips 100 KV EM208S) was utilized to evaluate the shape and size of sintered and non-sintered BAG nanopowders. The TEM images of powders were performed after 25 minutes ultrasonic in ethanol. The XRD pattern inwide-angle and small-angle using software Philips X'Pert-MPD diffracto-meter which operated at 35 KV and 40 mA using Cu $K_a$ radiation ($\lambda_1$ = 0.15418 nm) over the range of $20° \geq 2\theta \geq 55°$. The nanocrystalline size of BAG nanopowder before and after SPS process was determined using modified Scherrer Eq. (3) from the XRD pattern ns data.

$$ln\beta = ln(1/cos\ \theta) + ln(k\lambda/L) \quad (3)$$

The specific surface area of the NHA and BAG powders was obtained by N2 adsorption–desorption (Model ASAP 2010, Micro meritics, Norcross, GA) with multiple point's method.

The average particle size of samples were calculated according to the following Eq. (4),

$$D = \frac{6000}{S(BET) \times \rho} \quad (4)$$

## 4. Result and discussion

### *4.1. SEM analysis*

The surface morphology of nanocomposite powders which is sintered by SPS process reveals that it has non spheroid crystals; however, some non-spherical particles were seen while others have irregular shapes. Fig. 2 examinations revealed that the composite powder with different content of BAG maintained a highly porous structure with more than 45% pore interconnectivity (Fig. 2a-c).

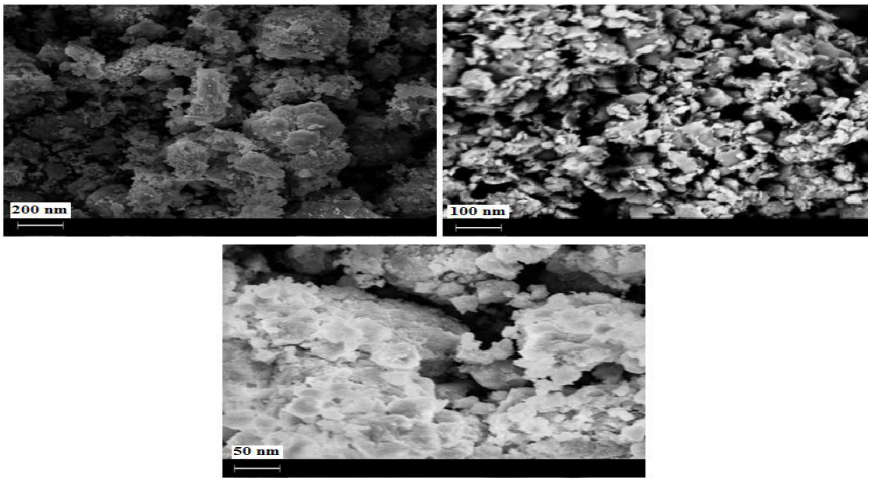


Fig. 2. Comparison of SEM micrograph of the sample containing (a) 10%, (b) 20%, and (c) 30% BAG after SPS for 2 hours.

### *4.2. XRD Analysis*

Figure 3 shows the crystallinity of powder and nanocomposite with different amount of BAG. The nanocrystalline size of the powders investigated after SPS process by XRD. The results show that sintering of BAG at 1350°C for 10 hours was adequate. By increasing BAG content to the NHA, the intensity of the peaks between $20° \geq 2\theta \geq 60°$ decreased. It seems that the formation of BAG phases between the NHA particles leads to the formation of amorphous region and leads to improve in density as shown in SEM section. As the BAG content increased up to 30%, the overlapping of glass bonds were observed more intense due to the presence of silicate ions in BAG as shown in Figure 4. The sintered BAG sample indicates sintering process has completed. From this figure, broader peaks were observed, BAG characteristic peaks gradually shifted to the right hand side.

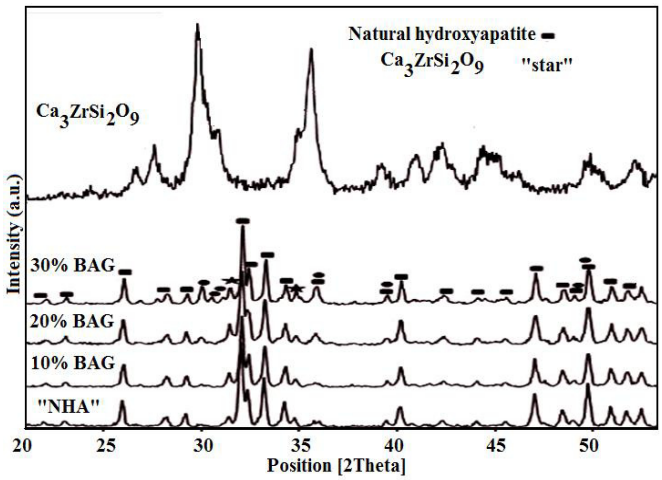


Fig. 3. Comparison of XRD patterns of the nanocomposites with different amounts of BAG (10 wt%, 20 wt%, and 30 wt.%).

### *4.3. BET Analysis*

The BAG powder density is 3.48 g/cm$^3$, while the diameter is 50 nm Eq. (4) and calculated BET result is 34.48 m$^2$/g.

### *4.4. Porosity determination*

The % porosity was obtained according to the Eq. (1) more than 65%. The % porosity is shown in table 2. The values of bulk density and % porosity of the samples confirm the formation of more compact structure with increased BAG content.

Table 2. Comparison of bulk density and % porosity of nanocomposites.

| Sample ID | Porosity (%) | Bulk density (g/cm$^3$) | CCS (MPa) | Youngs modulus (GPa) |
|---|---|---|---|---|
| BAG | 65 | -- | 1.6 | 90 |
| NHA | 60 | 3.2 | 1.3 | 85 |
| Nanocomposite 10 | 58 | 4.2 | 2.4 | -- |
| Nanocomposite 20 | 53 | 5.6 | 2.5 | -- |
| Nanocomposite 30 | 49 | 7.6 | 2.8 | -- |

### *4.5. CCS Determination*

As the NHA encounter with weak mechanical properties, the composite of NHA with BAG improved the CCS. A maximum value of 2.8 MPa was obtained for the compressive strength of S5. By increasing the amount of BAG up to 30 wt. %, bulk density starts to increase. This is attributed to the overlapping of glass bonds. The more increase in the degree of BAG content leads to improved mechanical strength and result in more compact structure as shown in table 2. Sintering process affects porosity and CCS of nanocomposites. From the SEM and CCS results, it is obvious that loose structure with high porosity weakens mechanical performance of materials.

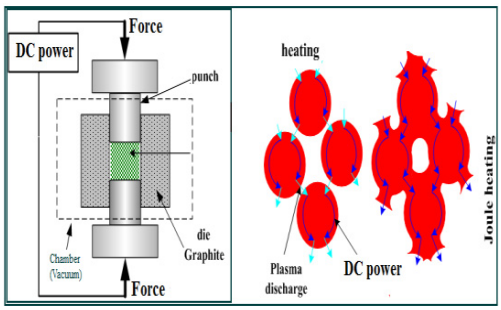


Fig. 4. Spark plasma sintering schematic presented with plasma discharge and joule heating event

## 5. Conclusion

The CCS results of nanocomposite are between 2.4-2.8 (GPa) which is exhibit better CCS result compared to S1 and S2. However, the superior mechanical performance of nanocomposite as well as the higher CCS and fracture toughness makes it a promising biomaterial using for tatal hip joint application. It can be concluded that improving the mechanical performance of BAG by adjusting the SPS processing is accessible. The CCS relate to many factors like type of material, the dimensions of the pores, pore channels and SPS condition. Increasing temperature leads to decreasing parameters of volume porosity, however increasing strength. Our findings indicate that the SPS of

nanocomposite possessed both excellent mechanical properties which make it appropriate candidate for orthopedic applications.

## References

Burchardt, H., 1983. The biology of bone graft repair. Clinical orthopaedics and related research 174, 28-34.

Finkemeier, C. G., 2002. Bone-grafting and bone-graft substitutes. The Journal of Bone & Joint Surgery 84(3), 454-464.

Farzadi, A., Bakhshi, F., Solati-Hashjin, M., Asadi-Eydivand, M., abu Osman, N. A., 2014. Magnesium incorporated hydroxyapatite: Synthesis and structural properties characterization. Ceramics International 40(4), 6021-6029.

Khandan, A., Karamian, E., Bonakdarchian, M., 2014. Mechanochemical synthesis evaluation of nanocrystalline bone-derived bioceramic powder using for bone tissue engineering. Dental Hypotheses 5(4), 155.

Karamian, E., Khandan, A., Eslami, M., Gheisari, H., Rafiaei, N., 2014. Investigation of HA nanocrystallite size crystallographic characterizations in NHA, BHA and HA pure powders and their influence on biodegradation of HA. In Advanced Materials Research 829, 314-318.

Khandan, A., Abdellahi, M., Barenji, R. V., Ozada, N., Karamian, E., 2015. Introducing natural hydroxyapatite-diopside (NHA-Di) nano-bioceramic coating.Ceramics International.

Lu, Z., Wang, G., Roohani-Esfahani, I., Dunstan, C. R., Zreiqat, H., 2013. Baghdadite ceramics modulate the cross talk between human adipose stem cells and osteoblasts for bone regeneration. Tissue Engineering Part A 20(5-6), 992-1002.

Ramaswamy, Y., Wu, C., Zhou, H., Zreiqat, H., 2008. Biological response of human bone cells to zinc-modified Ca–Si-based ceramics. Acta Biomaterialia 4(5), 1487-1497

Wu, C., Chang, J., 2004. Synthesis and apatite-formation ability of akermanite. Materials Letters 58(19), 2415-2417.